User Body Interaction of 5G Switchable Antenna System for Mobile Terminals at 28 GHz

Rodriguez Cano, Rocio; Zhang, Shuai; Zhao, Kun; Pedersen, Gert F.

Published in:
13th European Conference on Antennas and Propagation (EuCAP)

Publication date:
2019

Document Version
Accepted author manuscript, peer reviewed version

User Body Interaction of 5G Switchable Antenna System for Mobile Terminals at 28 GHz

Rocío Rodríguez-Cano[1], Shuai Zhang[1], Kun Zhao[1-2], Gert F. Pedersen[1]
[1]Antenna, Propagation and Mm-Wave Systems Section (APMS), Department of Electronic Systems, Aalborg University, Aalborg, Denmark
[2]Research and Standardization, Sony Mobile Communications, Lund, Sweden
{*rrc, sz, kz, gfp*}*@es.aau.dk*

***Abstract*—In this paper, a 12-element switchable antenna system for handsets is proposed at 28 GHz. The effect of the head and hand in the impedance matching and radiation pattern is assessed. The electromagnetic field (EMF) exposure in the body is analyzed. The evaluation method of exposure for the previous mobile generations is the specific absorption rate (SAR). Since the penetration depth of the EMFs is lower at the millimeter-wave (mm-wave) band, power density (PD) in free space is employed as evaluation metric instead. The maximum permissible transmitted power to satisfy the proposed limits is calculated, showing a severe discontinuity compared with the maximum power in 4G UE. The exposure of the switchable monopole is compared with a patch phased array, showing a faster decrease in the PD peak than the array at 1.3 cm from the terminal.**

***Index Terms*—5G mobile communication, antenna array, RF EMF exposure, power density, handset.**

I. Introduction

Wireless devices emitting radio frequency (RF) electromagnetic fields (EMFs) impact differently on the body according to the operating frequency band and, thus, require different protection regulations. With the saturation of the spectrum under 3 GHz, the upcoming fifth generation (5G) of mobile communications is planning to extend to the millimeter-wave (mm-wave) bands [1]–[3]. The guidelines for RF EMF exposure are provided either by the International Commission of Non-Ionizing Radiation Protection (ICNIRP) [4] or by the U.S Federal Communications Commission (FCC) [5]. The Institute of Electrical and Electronics Engineers (IEEE) has also specified a set of exposure limits, but they have not been adopted by any regulations yet. For the former generations of mobile communications, the exposure metric is the specific absorption rate (SAR), expressed in (W/kg). For frequencies higher than 3 GHz (IEEE), 6 GHz (FCC) and 10 GHz (ICNIRP), the exposure metric changes from SAR to free-space power density (PD), in W/m^2. The spatial peak value of the PD set by the FCC is 10 W/m^2, although the results of the spatial peak depend on the assessment method. FCC has also proposed PD limits for an averaging area of 1 cm^2, but it has not been adopted yet. ICNIRP specifies a value of 10 W/m^2 taken as a spatial average over any 20 cm^2 of exposed area. IEEE averages the power density over any contiguous $100\lambda^2$ area, where λ is the free-space wavelength. The power density levels will affect the maximum permissible transmitted power (MPTP) in 5G. In [6], the maximum power for a half-wavelength dipole is calculated at a distance of 2 cm to be in compliance with FCC and ICNIRP. The maximum radiated power for long term evolution (LTE) is 23 dBm. However, for the half-wavelength dipole above 6 GHz for FCC and 10 GHz for ICNIRP, the maximum power should be reduced to 15 dBm and 18 dBm, respectively, which is lower than the current value.

The placement of the new mm-wave antenna arrays in an already crammed space presents a major challenge in the design of mobile terminals. Moreover, the signal level is also dependent on the body effect and how the user holds the phone. Authors in [7] show that the best performance of the antenna system in terms of spatial coverage with user effects can be obtained when the array is located at the corners of the printed circuit board (PCB).

In this paper, a 12-element switchable corner antenna system is proposed at 28 GHz. Each 3-element sub-array can be plugged in the corners of the phone. RF EMF exposure of the mm-wave antenna system is assessed at 28 GHz and the maximum output power is obtained to meet the provisional limitations. Simulations are performed with the commercial electromagnetic software CST Microwave Studio 2018.

II. Antenna System Design

The antenna configuration is shown in Fig. 1 (a). The system is composed of 12 switchable top-loaded monopoles with reflector distributed along the corners of a phone PCB to ensure 3D-coverage. The PCB dimensions are 60 mm $\times$ 120 mm. The overall dimensions of each antenna module are 5 mm $\times$ 5 mm $\times$ 10 mm. Each corner sub-array is composed of 3 antennas, which can be switched. The sub-arrays are designed to form an L-shaped module that can easily be embedded in the corners of the PCB. Adding a top load decreases the physical length of the monopole. Since the system is supposed to switch between the elements, each monopole needs high gain. For that reason, a reflector is added, and the length of the monopole is enlarged $\lambda/2$.

III. User Body Effect

The reflection coefficient of the antenna system is represented in Fig. 2 (port numbering is shown in Fig. 1 (a)). Port 1

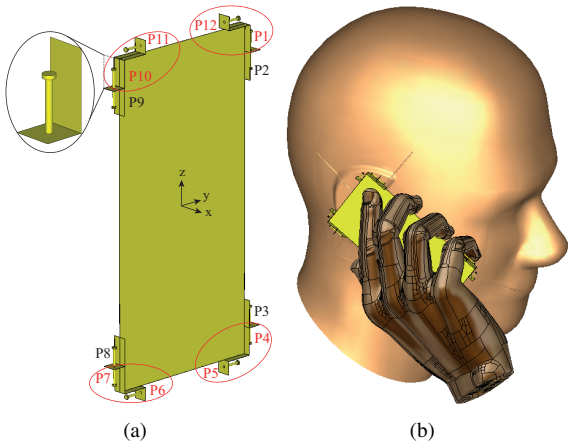

Fig. 1. Simulated models. (a) Antenna system with a zoomed view of the top-loaded monopole. (b) Hand and head phantom.

is not covered by any finger and the S_{11} is practically identical when the antenna system is simulated alone and when the head and hand phantoms are added. In the case of port 7, the little finger is slightly covering the bottom part of the antenna module, but without touching the antenna. This placement of the finger produces a small detuning of the resonance to higher frequencies, but the reflection coefficient of the port is still under -10 dB at 28 GHz. Finally, in the case of port 8, the little finger is touching the monopole, which produces a mismatching of the port. This position of the finger would not be possible in the real prototype, since the phone casing would protect the antenna. However, it is included in order to fully assess all the possibilities.

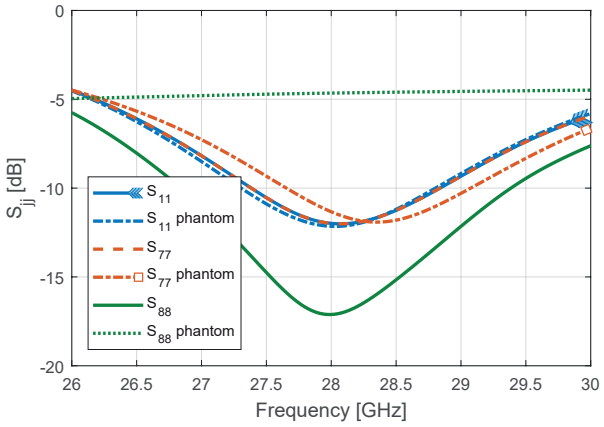

Fig. 2. Reflection coefficient comparison of the antenna only and the antenna with head and hand.

The total radiation pattern corresponds to the maximum gain achieved by any of the antennas at each point of the sphere and it is shown in Fig. 3. In Fig. 3(a)-(b), there is no combination of the radiation patterns of the antenna elements. The effect of the fingers and head can be seen in Fig. 3 (b), the radiation pattern becomes more directive with the phantom, and therefore it reaches a maximum of 12.8 dBi, 4 dB higher than the antenna system in free-space. Fig. 3(c)-(d) correspond to the combination of several ports. This means that the ports combined together in a corner act like a single element to obtain the total radiation pattern. In the legend of Fig. 3 and Fig. 4, it is only specified the antenna combination of one corner, but its other corner counterparts are also considered. For example, if port 1 and 12 are combined, it means that the pairs 4 and 5, 6 and 7, and 10 and 11 are combined as well. Each corner combination is marked in red in Fig. 1 (a). With this combination, the gain of the antenna system in free-space increases to 10.6 dBi and when the phantom is added, up to 13.9 dBi.

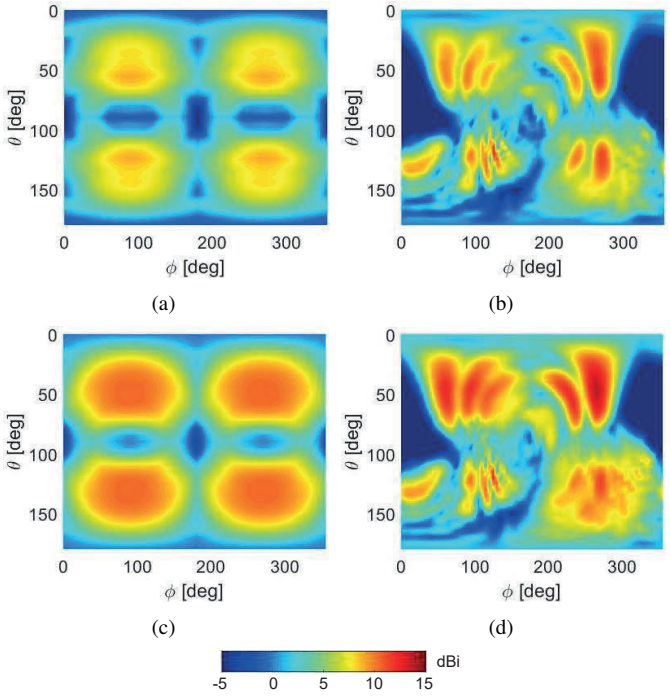

Fig. 3. Total radiation pattern comparison. The first column corresponds to the radiation pattern in free space, while the second column includes the hand and head effects. (a) and (b) represent the radiation pattern with no element combination. (c) and (d) include the combination of ports 1 and 12.

Even if the gain increases due to the user effects, the spherical coverage [8] is lower in that case. The coverage efficiency of the antenna system is represented in Fig. 4. The 50 % coverage efficiency of the antenna array in free-space can be increased 2.5 dB if the two ports of each corner sub-array are combined. The increase is only 1.5 dB in the case of including the effects of the head and hand.

IV. RF EMF Exposure

The exposure evaluation metric at the mm-wave band varies from the specific absorption rate to power density. The time-averaged power density (Poynting vector) can be obtained as

$$\mathbf{S}(x,y,z) = \frac{1}{2} Re[\mathbf{E}(x,y,z) \times \mathbf{H}^*(x,y,z)] \qquad (1)$$

in which $\mathbf{S}$ denotes the time-averaged power density, $\mathbf{E}$ the electric field and $\mathbf{H}$ the magnetic field. To obtain the maximum

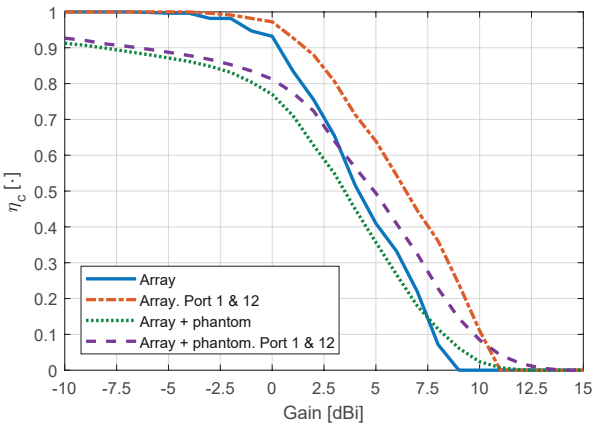

Fig. 4. Coverage efficiency comparison.

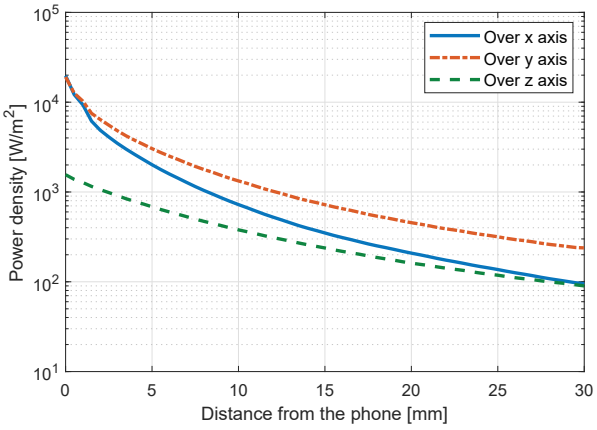

Fig. 5. Peak PD comparison of a single element at planes perpendicular to the different axis.

PD averaged over any square-shaped area, A_{av}, in a plane $x = d$ (coordinates in Fig. 1 (a)) [9],

$$S_{av}(x = d) = \max_{y,z} [\frac{1}{A_{av}} \iint_{A_{av}} \mathbf{S}(d, y, z)\, \hat{x}\, dy\, dz\,]. \quad (2)$$

The power density in free-space has been evaluated in terms of the spatial peak and spatially averaged metrics of FCC and ICNIRP. The total radiated power of the antenna element is normalized to 23 dBm. Fig. 5 shows the PD above the different axes. The element excited is number 1 (see Fig. 1 (a)). It can be seen that the peak PD is higher when the distance is measured over the y axis. From now on, the PD of the monopole is shown at a distance along the y axis. The PD of a single element of the antenna system as a function of the distance above the PCB plane is represented in Fig. 6 (a). The lower PD is obtained when the averaging area is 20 cm^2. The patch array in Fig. 7, is simulated as well in order to compare the EMF exposure between the switchable antenna array and a phased array. In the case of the patch, the higher power density is obtained along the x axis. Fig. 6 (b) shows that the peak PD of a patch array is lower than the PD of the monopole in the reactive near-field. This is due to the fact that larger array apertures lower the peak value, considering that the radiated power of patch array and monopole is the same. Further away from the phone, the PD of the array decreases slower than a single element.

The maximum permissible transmitted power can be calculated from the PD and it is defined in [9] as

$$MPTP(d) = \frac{P_s S_{lim}}{S_{max}(d)} \quad (3)$$

where d is the distance of evaluation above the array, P_s is the total radiated power, S_{lim} is the power density limit (in this case 10 W/m^2) and S_{max} is the spatial peak PD. The maximum permissible transmitted power of a single element to achieve a power density limitation of 10 W/m^2 is obtained in Fig. 8 (a) as a function of the distance. The maximum power should be 6.4 dBm, 10 dBm and 12.4 dBm, respectively for the spatial peak, 1 cm^2 and 20 cm^2 averaging area, at a distance of 2 cm to respect the provisional regulations. The lowest permissible power is 16.6 dBm less than the current limitation for 4G user equipment. This aligns with the results obtained in [6], [9], [10]. The peak MPTP comparison of the switchable antenna system and the patch phased array is compared in Fig. 8 (b). At a distance of 1.3 cm, the maximum power of the monopole overpasses the patch array, reaching a level of 10 dBm at 2 cm.

V. Conclusion

A mm-wave 12-element switchable antenna system is proposed for simple integration at the corners of the handset. The effects of the hand and head in the radiation pattern are analyzed, resulting in a more directive total scan pattern but with lower coverage efficiency. The gain is also enhanced with the combination of 2 out of the 3 available ports per corner.

In order to obtain the EMF exposure results at 28 GHz, the power density of the antenna system is assessed as a function of the distance above the PCB. With the power density it is possible to calculate the maximum permissible transmitted power by each antenna in order to meet the provisional requirements. As the figures show, with a limitation of 10 W/m^2, there should be a big discontinuity between the maximum power in LTE and mm-wave, which would increase the complexity of the integrated system. Exposure of the switchable antenna element is compared with a phased array, showing that the larger aperture of the phased array presents lower power density close to the terminal, but then decreases slower than the monopole element as the distance augments.

Acknowledgment

This work was supported by the InnovationsFonden project of Reconfigurable Arrays for Next Generation Efficiency (RANGE).

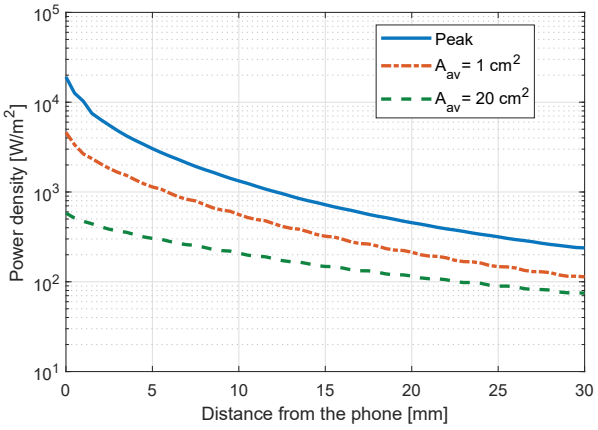

(a)

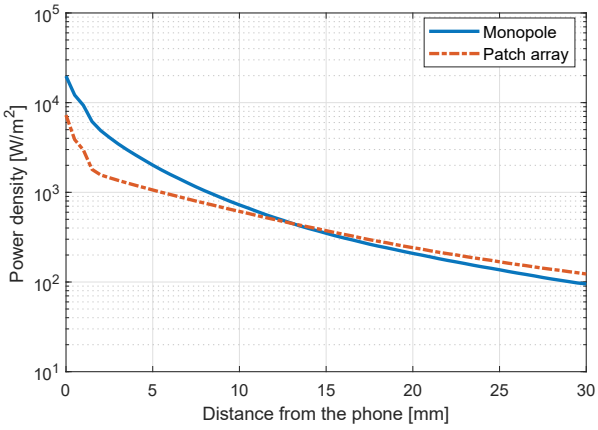

(b)

Fig. 6. (a) Power density of a single antenna element as function of the distance d above the PCB plane (in the x axis). (b) Peak PD comparison of a single element of the top-loaded monopole and the patch array in Fig. 7.

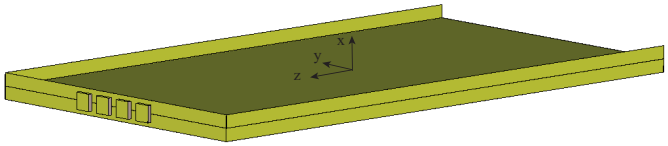

Fig. 7. Vertically polarized patch phased array.

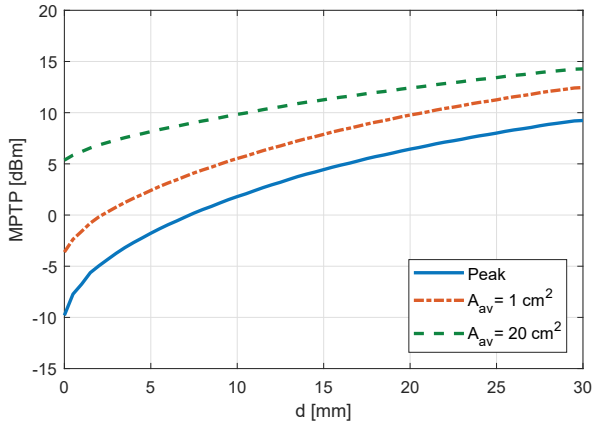

(a)

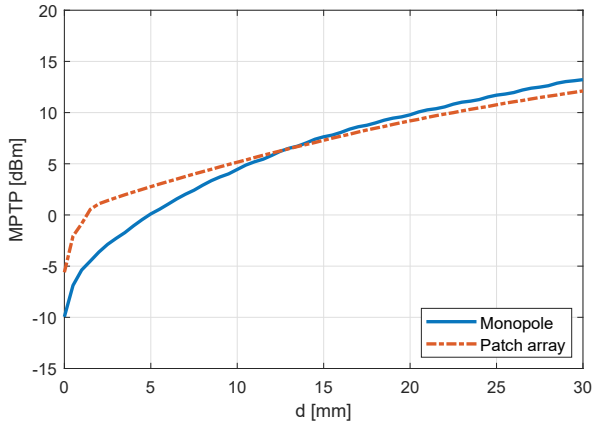

(b)

Fig. 8. (a) MPTP as function of the distance d above the PCB plane (in the x axis). (b) Peak MPTP comparison of a single element of the top-loaded monopole and the patch array.

REFERENCES

[1] T. S. Rappaport, S. Sun, R. Mayzus, H. Zhao, Y. Azar, K. Wang, G. N. Wong, J. K. Schulz, M. Samimi, and F. Gutierrez, "Millimeter wave mobile communications for 5g cellular: It will work!" *IEEE Access*, vol. 1, pp. 335–349, 2013.

[2] Z. Pi and F. Khan, "An introduction to millimeter-wave mobile broadband systems," *IEEE communications magazine*, vol. 49, no. 6, 2011.

[3] J. Lee, E. Tejedor, K. Ranta-aho, H. Wang, K.-T. Lee, E. Semaan, E. Mohyeldin, J. Song, C. Bergljung, and S. Jung, "Spectrum for 5g: Global status, challenges, and enabling technologies," *IEEE Communications Magazine*, vol. 56, no. 3, pp. 12–18, 2018.

[4] I. C. on Non-Ionizing Radiation Protection, "Guidelines for limiting exposure to time-varying electric, magnetic, and electromagnetic fields (up to 300 ghz)," *Health physics*, vol. 97, no. 3, pp. 257–258, 2009.

[5] F. C. Commission *et al.*, "Code of federal regulations cfr title 47, part 1.1310," *Washington, DC: FCC*, 2010.

[6] D. Colombi, B. Thors, and C. Törnevik, "Implications of emf exposure limits on output power levels for 5g devices above 6 ghz," *IEEE Antennas and Wireless Propagation Letters*, vol. 14, pp. 1247–1249, 2015.

[7] I. Syrytsin, S. Zhang, G. F. Pedersen, and A. Morris, "Technique of user shadowing suppression for 5g mm-wave mobile terminal antennas," (submitted to IEEE Transactions on Antennas and Propagation).

[8] J. Helander, K. Zhao, Z. Ying, and D. Sjöberg, "Performance analysis of millimeter-wave phased array antennas in cellular handsets," *IEEE Antennas and wireless propagation letters*, vol. 15, pp. 504–507, 2016.

[9] B. Xu, K. Zhao, B. Thors, D. Colombi, O. Lundberg, Z. Ying, and S. He, "Power density measurements at 15 ghz for rf emf compliance assessments of 5g user equipment," *IEEE Transactions on Antennas and Propagation*, vol. 65, no. 12, pp. 6584–6595, 2017.

[10] B. Thors, D. Colombi, Z. Ying, T. Bolin, and C. Törnevik, "Exposure to rf emf from array antennas in 5g mobile communication equipment," *IEEE Access*, vol. 4, pp. 7469–7478, 2016.